

## Optimization of base crystals for silicon solar cells of various destinations

*M.V.Kirichenko, I.T.Tymchuk<sup>\*</sup>, V.A.Antonova<sup>\*</sup>,  
N.P.Klochko, V.R.Kopach, A.M.Listratenko<sup>\*</sup>*

National Technical University "Kharkiv Polytechnical Institute",  
21 Frunze St., 61002 Kharkiv, Ukraine

<sup>\*</sup>State Enterprise "Research and Development Technological Institute for  
Instrument Engineering", 40/42 Primakov St., 61010 Kharkiv, Ukraine

*Received January 9, 2007*

The spectral dependences of reflection coefficient  $R(\lambda)$  for various light-receiving surface texture types ("inverted pyramids" and "V-grooves") of single crystal silicon wafers are presented as well as output and diode parameters of solar cells (SC) with  $p$ - and  $n$ -type silicon base crystals (Si-BC). Basing on comparative analysis of  $R(\lambda)$  dependences, the selection of an optimum type of Si-BC light-receiving surface texture is substantiated. Comparing the output and diode parameters of SC with Si-BC of  $p$ - and  $n$ -type conductivity, the development expediency of high-efficiency Si-SC with the  $n$ -type conductivity single crystals is substantiated.

Приведены результаты исследований спектральной зависимости коэффициента отражения  $R(\lambda)$  для различных типов текстуры ("инвертированные пирамиды" и "V-канавки") фотоприемной поверхности монокристаллических кремниевых пластин, а также выходных и диодных параметров фотоэлектрических преобразователей (ФЭП) с базовыми кристаллами кремния (Si-БК)  $p$ - и  $n$ -типа проводимости. На основании проведенного сравнительного анализа зависимостей  $R(\lambda)$  обоснован выбор оптимального вида текстуры фотоприемной поверхности Si-БК для отечественных ФЭП космического и наземного применения. Путем сопоставления выходных и диодных параметров ФЭП с Si-БК  $p$ - и  $n$ -типа проводимости обоснована целесообразность создания высокоэффективных отечественных монокристаллических Si-ФЭП наземного применения на основе кремния  $n$ -типа проводимости.

The increasing need for environment-friendly and high-efficiency energy sources stipulate the swift acceleration in the field of improvement and manufacture of solar energy photovoltaic converters — solar cells (SC). Taking into consideration the trends at the third millennium beginning [1], the production of single crystal Si-SC to year 2010 should be not less than 30 % of total world SC production, which is equivalent to peak power about 5.4 GW/year [2, 3]. The main requirements to this kind of SC will be the increasing efficiency ( $\eta$ ), mass-power performance  $P_M^*$  (maximum useful power

produced by SC referred to its mass), and durability.

The serial  $p$ -type single crystal Si-SC with base crystals (BC) thickness  $t = 300 \pm 50 \mu\text{m}$  have an efficiency  $12 < \eta \leq 14$  % and  $200 < P_M^* < 275$  W/kg at 25°C in the conditions of solar spectrum outside the Earth atmosphere (AM0 regime) and  $15 \leq \eta \leq 16$  % and  $170 < P_M^* < 230$  W/kg in terrestrial conditions — on the Earth surface when the sun is positioned at 45° above horizon (AM1,5 regime). However, they are inferior in the indicated parameters to the best foreign analogues having, for example,  $\eta \approx 21$  %

(AM0) and  $\eta \approx 25\%$  (AM1,5) at comparable  $t$  values [4]. Therefore, increasing of domestic Si-SC efficiency remains an actual problem.

There are several real ways to solve this problem basing on development of an effective light-trapping system of photoelectric active component of sunlight by the BC; optimization of BC thickness; and recombination losses reduction within the SC BC bulk, on its back and front surfaces in as-prepared state as well as at consequent radiation and photon effects.

The major design component necessary for development of an effective system for light trapping by base crystal is the textured front surface [5]. In the BC thickness optimization course, it provides a considerable increase in the photocurrent density  $J_{ph}$ , and, hence, in efficiency and  $P_M^*$  [5, 6]. The recombination loss level in Si-BC depends essentially on the type and concentration of the main dopant [7–9]. Therefore, to solve the above-mentioned problem, the sunlight reflection coefficient  $R(\lambda)$  spectral dependences in the 0.4–0.8  $\mu\text{m}$  wavelength range was studied in this work for various light-receiving front surface texture types of (100) oriented Si-BC, as well as the output and diode parameters of Si-SC depending on the conductivity type and doping level of BC.

The texturing methods developed to date provide formation of various texture types on silicon crystal surface: a random texture with lugs such as pyramids or cones and ordered texture shaped as "inverted (submerged) pyramids (IP)", "V-grooves" (VG) or submerged cones [5, 7, 8]. According to experimental data, the highest efficiency is attained at the "inverted pyramids" (IP) and "V-grooves" (VG) textures, providing  $R \leq 1\text{--}2\%$  at  $0.5 \leq \lambda \leq 1.0 \mu\text{m}$  after deposition of bilayer antireflection coating onto the textured surface [8].

Until recently, at development and manufacture of single crystal Si-SC with  $p$ - $n$  homojunction, the  $p$ -type Si-BC were preferred because of higher mobility  $\mu_n$  of minority charge carriers (electrons), and consequently their diffusion lengths  $L_n$ , in contrast to similar parameters ( $\mu_p$  and  $L_p$ ) for holes in  $n$ -type Si-BC. This is known [6] to promote increased initial  $J_{ph}$  value and enhanced stability of Si-SC with  $p$ -type BC against high-energy electrons and protons in space. At the same time, competitiveness of Si-SC with  $n$ -type BC under considerable

influence of surface recombination processes on Si-SC parameters has been theoretically substantiated [7]. As shown in [7], the use of  $n$ -type Si-BC with thin base ( $t < L_p$ ) should provide reduction of Si-SC diode saturation current density  $J_0$  approximately by a factor of 3 as compared to Si-SC with  $p$ -type BC. The  $J_0$  reduction might result in increased open circuit voltage  $U_{OC}$  and consequently [6] the Si-SC efficiency.

As Si-SC with  $n$ -type BC are more sensitive to crystal lattice damages appearing in space due to high-energy particles irradiation than Si-SC with  $p$ -BC [6], the area of their application should be limited to terrestrial application. However, in this case, they can differ favourably from Si-SC with  $p$ -type BC not only in the initially higher efficiency, but also in absence of photon degradation effect [10, 11]. For Si-SC with  $p$ -type BC traditionally doped with boron, the mentioned effect is amplifying catastrophically with increasing of boron atomic concentration  $N_B$  from  $10^{15} \text{ cm}^{-3}$  up to  $10^{17} \text{ cm}^{-3}$ . So, for example, at  $N_B \sim 10^{16} \text{ cm}^{-3}$  (resistivity  $\rho \sim 1 \Omega\cdot\text{cm}$ ), the photon degradation results for minority carrier lifetime decrease in the bulk of  $p$ -type Si-BC from 100  $\mu\text{s}$  down to 10  $\mu\text{s}$ , that is the reason of  $U_{OC}$  reduction approximately by 4–5 % [10, 11]. Therefore, for space Si-SC, the  $p$ -type BC with  $N_B \approx 1.5 \cdot 10^{15} \text{ cm}^{-3}$  and  $\rho \approx 10 \Omega\cdot\text{cm}$  are used [12], where the photon degradation of Si-SC is less essential.

In connection with the above, the investigations on optimization of Si-BC front surface relief geometry with "inverted pyramids" (IP) and "V-grooves" (VG) textures as well as on experimental comparison of output and diode parameters of Si-SC with  $p$ - and  $n$ -type BC have been realized.

The experimental samples with textured surface were manufactured from (100) oriented SHB-10 silicon wafers. The surface was textured through the windows formed by photolithography in  $\text{SiO}_2$  mask layer using the process described below.

A protective  $\text{SiO}_2$  layer was formed on the polished surface and opposite grinded surface of a silicon wafer. Then the windows of various geometrical sizes were opened by photolithography and etching at the polished surface side. Thereafter, the wafer was immersed in hot 10–20 wt.% KOH solution where selective chemical etching of silicon was carried out through the mentioned windows in  $\text{SiO}_2$ . Thus, inverted pyramids were formed at the side of pol-

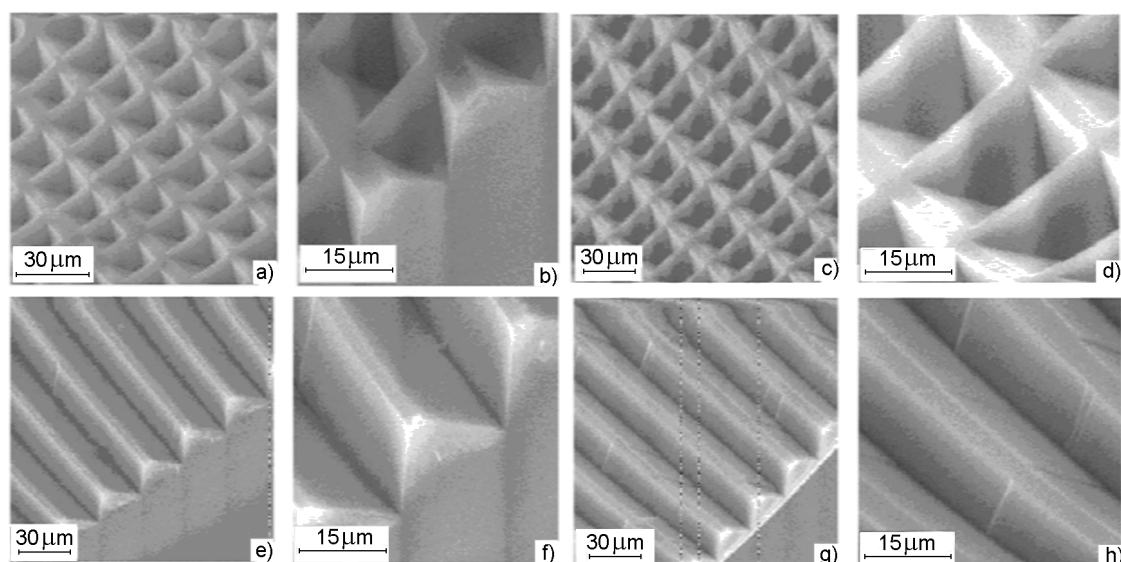


Fig. 1. Texture of "inverted pyramids" (IP) type in samples 1-IP (a, b), 2-IP (c, d) and texture of "V-grooves" (VG) type in samples 3-VG (e, f), 4-VG (g, h).

ished surface, limited by (111) crystallographic planes. Using this process, 1-IP and 2-IP samples were obtained. In a similar manner, 3-VG and 4-VG samples with V-grooves were made with inclined surfaces representing also (111) crystallographic planes. However, for this purpose, extended windows of different widths were opened in  $\text{SiO}_2$  layer before etching at the side of wafer polished surface.

Data on the texture element sizes for the above samples are presented in Table 1. Here,  $b$  is the pyramid base or the groove width;  $d$ , step of pyramids or grooves arrangement;  $S_M$ , the non-etched fraction of frontal surface area for front metal fingers;  $S_N$ , the non-etched fraction of frontal surface area between pyramids or grooves.

To determine the optimum front surface texture type, the silicon wafers with various texture types were studied using optical and electron microscopy. The sample photos obtained in a REM-100U scanning electron microscope are shown in Fig. 1. As is seen from Table 1, samples of the same texture

types (1-IP, 2-IP and 3-VG, 4-VG) differ in the polished non-textured surface areas including the areas between pyramids and grooves, and also non-textured surface for metal fingers.

For comparison purposes and for well-substantiated choice of optimum texture type, the  $R(\lambda)$  measurements for investigated samples were carried out by an SF-18 spectrophotometer.

To compare the Si-SC output and diode parameters depending on the Si-BC conductivity type and doping level, the SC laboratory samples of 350–380  $\mu\text{m}$  Si-BC thickness and the planar surface area 2.25  $\text{cm}^2$  (one of which (frontal) was polished, and other (back), grinded) were investigated. The  $p$ -type BC were doped with boron, and were cut out from single crystal SHB-10 silicon ingots ( $\rho \approx 10 \Omega\cdot\text{cm}$ ) grown by Czochralski technique. The  $n$ -type BC were doped with phosphorous, and were cut out from single crystal SNE-2 silicon ingots ( $\rho \approx 2 \Omega\cdot\text{cm}$ ) grown by crucible-free zone melting.

The appearance of investigated samples with grid metallization at the front surface is shown in Fig. 2. The Si-SC with  $p$ -type BC had  $n^+p-p^+$  diode structure, but Si-SC with  $n$ -type BC had  $p^+-n-n^+$  one. Diffusive  $n^+$ - and  $p^+$ -layers were doped with phosphorous and boron, respectively, up to a level of  $10^{19}$ – $10^{20} \text{ cm}^{-3}$ , and their thickness was 0.6–0.8  $\mu\text{m}$ . The SC electrode at the  $n^+$ -layer side consisted of contacting titanium layer of 0.1  $\mu\text{m}$  thickness coated with 2  $\mu\text{m}$

Table 1. Types and parameters of textures.

Sample	1-IP	2-IP	3-VG	4-VG
Texture types	Inverted pyramids	Inverted pyramids	V-type grooves	V-type grooves
$b$ , $\mu\text{m}$	16	24	24	16
$d$ , $\mu\text{m}$	24	32	32	24
$S_M$ , %	7.3	7.3	7.3	7.3
$S_N$ , %	55.6	43.8	25.0	33.4

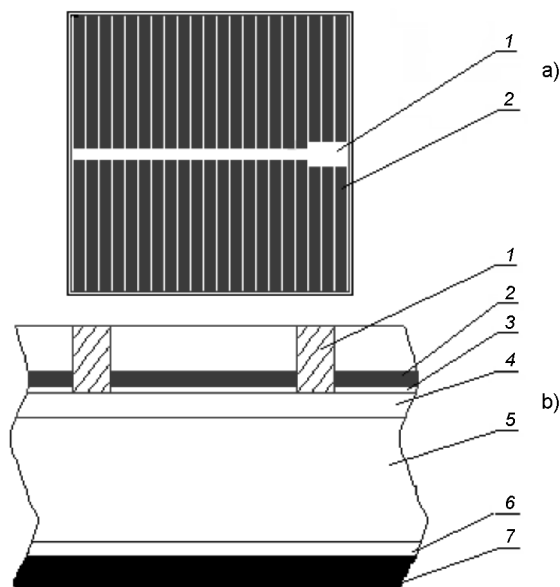


Fig. 2. Schematic image of investigated SC design with  $n^+p-p^+$  and  $p^+n-n^+$  diode structures: (a), illuminated frontal surface with planar dimensions  $15 \times 15 \text{ mm}^2$  (1, grid frontal electrode consisting of a bar connecting  $2 \times 21$  parallel fingers; 2, antireflection  $\text{TiO}_2$  coating); (b) — a part of SC section profile normal to SC frontal surface (3, passivating  $\text{SiO}_2$  layer; 4, diffusive  $n^+(p^+)$ -type layer; 5, silicon base crystal of  $p(n)$ -type conductivity; 6, diffusive  $p^+(n^+)$ -type layer; 7, back solid electrode).

thick aluminium layer. From the  $p^+$ -layer side, the electrode was made from aluminium of  $2 \mu\text{m}$  thickness. The back electrode was solid.

The load current  $I$  vs voltage  $V$  characteristics (IVC) of investigated SC were measured similarly to [13] at  $25^\circ\text{C}$  under the sample frontal surface irradiation power of  $1360 \text{ W/m}^2$ , that corresponds to the AM0 regime. The SC output and diode parameters were determined by analytical computer processing of measured IVC using the method described in [14].

The measured  $R(\lambda)$  dependences for sample textured surfaces are shown in Fig. 3. For comparison,  $R(\lambda)$  of silicon wafer ("PolishSi") with polished and non-textured surfaces are also presented.

It is seen from the presented dependences that the investigated samples have the following reflection coefficients  $R$  values (at  $\lambda = 600 \text{ nm}$ ): 1-IP, 26.2 %; 2-IP, 25.3 %; 3-VG, 19.4 %, 4-VG, 20.6 %. The lowest reflection coefficient (19.4 %) has the 3-VG sample with "V-grooves" textured

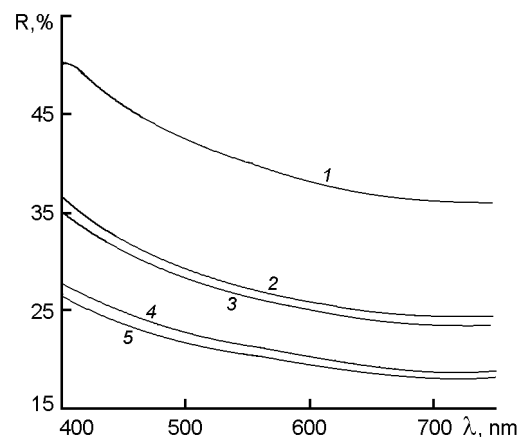


Fig. 3. Experimental spectral dependences of diffuse reflection coefficient for investigated samples with various texture types of frontal surface: 1, "PolishSi" (silicon wafer with polished and non-textured surfaces); 2, 1-IP; 3, 2-IP; 4, 4-VG; 5, 3-VG.

front surface at the groove width of  $24 \mu\text{m}$ , and the highest one (26.2 %), the 1-IP sample with the "inverted pyramids" texture at the base size of  $16 \times 16 \mu\text{m}^2$ .

Since a considerable fraction of the investigated sample surface area was non-textured (Table 1), the relevant analytical processing of obtained spectral dependences of a diffuse-reflection coefficient was carried out to eliminate its influence. The spectral dependences of diffuse reflection coefficient for the samples taking into account the analytical processing are shown in Fig. 4. Here, curves 1 are experimental  $R(\lambda)$  dependences; 2, calculated  $R(\lambda)$  dependences disregarding the non-textured areas for metal fingers; 3,  $R(\lambda)$  dependences disregarding of non-textured areas between pyramids and grooves.

The analytical processing results show the lowest reflection coefficient  $R \leq 5 \%$  in the whole wavelength range and  $R \approx 2 \%$  in the  $630 \leq \lambda \leq 750 \text{ nm}$  range for the "inverted pyramids" texture (1-IP sample) with the pyramid base size of  $16 \times 16 \mu\text{m}^2$ . Since the sample 1-IP has the greatest non-etched area (55.6 %), it cancels the advantage of the small inverted pyramids to form an effective light-trapping system for Si-SC base crystals.

The sample 3-VG, initially being best in integrated  $R$  value, after analytical data processing has the highest reflection coefficient  $7 < R \leq 10 \%$  in the whole examined spectral range. This is due to that the sample 3-VG has the non-etched area 25 % and

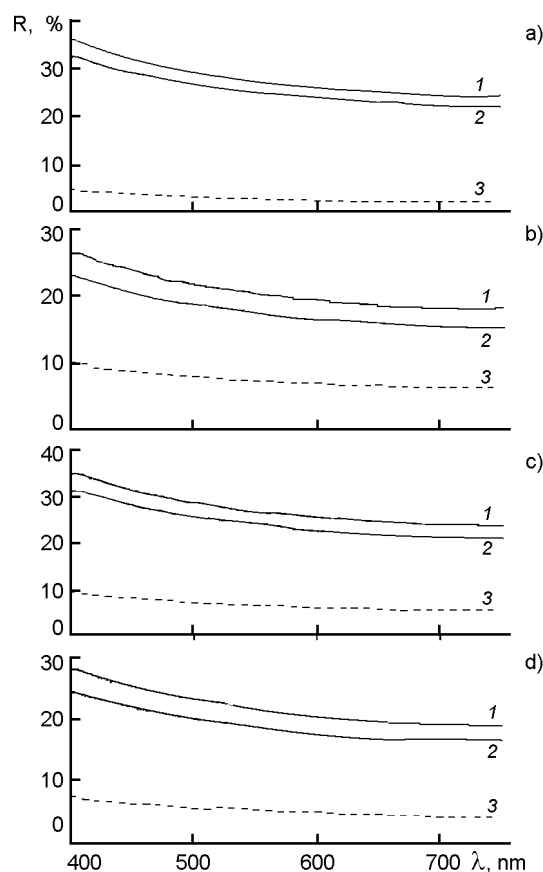


Fig. 4. Calculated dependences of diffuse reflection coefficient for investigated samples 1-IP (a), 2-IP (b), 3-VG (c) and 4-VG (d) after elimination of non-textured area contribution: 1, experimental  $R(\lambda)$  dependences; 2, calculated  $R(\lambda)$  dependences without contribution of non-textured regions for grid electrode; 3,  $R(\lambda)$  dependences without contribution of non-textured regions between pyramids and grooves.

this is the smallest as compared to similar areas of other investigated samples, thus providing the lowest experimentally registered reflection coefficient and results in a maximum loss in  $R(\lambda)$  after removal of the contribution from non-etched polished wafer surface into  $R(\lambda)$ . Thus, the "V-grooves" texture is optically less perfect compared to "inverted pyramids" texture.

The experimental IVC typical for all investigated Si-SC with  $p$ - and  $n$ -type BC after their preliminary repeated long-term irradiation at AM0 are shown in Fig. 5 numbered as 1 and 2, respectively. The values of output parameters: short circuit current density  $J_{SC} \approx J_{ph}$ , open circuit voltage  $U_{OC}$  and efficiency ( $\eta$ ) as well as diode parameters:

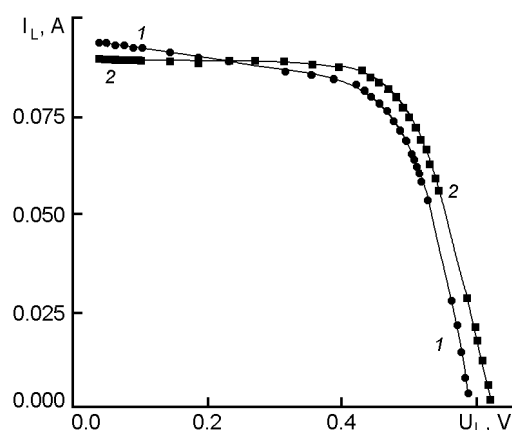


Fig. 5. Load IVC of investigated Si-SC: 1, with  $p$ -type BC; 2, with  $n$ -type BC.

Table 2. Parameters of investigated Si-SC.

IVC of SC	1	2
$J_{SC}$ , mA/cm <sup>2</sup>	42	40
$U_{OC}$ , mV	592	625
$\eta$ , %	12	13
$J_0$ , A/cm <sup>2</sup>	$9.4 \cdot 10^{-10}$	$2.7 \cdot 10^{-10}$
$A$ , rel. un.	1.4	1.3

ters: diode saturation current densities  $J_0$  and diode ideality factor  $A$ , typical for the samples, are presented in Table 2.

The comparison of Si-SC output and diode parameters presented in Table 2 testifies what follows. According to [6],

$$\eta \sim J_{SC} U_{OC}, \quad (1)$$

$$U_{OC} \approx \frac{AkT}{e} \ln \frac{J_{ph}}{J_0}, \quad (2)$$

(where  $k$  is Boltzmann constant;  $T$ , temperature;  $e$ , electron charge).

Thus, the higher efficiency of Si-SC with  $n$ -type BC is due obviously to higher  $U_{OC}$  value, which in turn is caused by reduced  $J_0$  level.

It is to note that for Si-SC with  $n$ -type BC, the  $J_0$  value is approximately 3.5 times less than for those with  $p$ -type BC. This is in a rather good agreement with theoretically substantiated competitiveness of Si-SC with  $n$ -type BC caused by approximately 3 times smaller  $J_0$  as compared to Si-SC with  $p$ -type BC [7]. In [7], that effect is related to reduced surface recombination rate of minority carriers in  $n$ -type BC. As it is seen

from Table 2, the diode ideality factor for Si-SC with  $n$ -type BC is lower than for those with  $p$ -type BC. This circumstance is an additional experimental argument for the slowing of surface recombination when passing from  $p$ -type BC to  $n$ -type BC.

Thus, the investigations of reflection coefficient spectral dependences for various Si-SC front surface texture types and analysis of obtained results have shown that the optimum texture is that of inverted pyramids with  $16 \times 16 \mu\text{m}^2$  pyramid base. At removal non-etched sites between the neighboring pyramids, this type of texture can provide reduction of the integrated reflection coefficient of a photoactive solar radiation component from the base silicon crystals frontal surface without antireflecting coating down to 2–3 %. It has been confirmed experimentally that when passing from boron doped  $p$ -type silicon BC with a resistivity 10 Ohm·cm to phosphorus doped  $n$ -type BC with resistivity 2 Ohm·cm (other elements of the Si-SC construction-technological solution (CTS) remaining unchanged) results in a noticeable decreasing of the diode saturation current density thus making it possible to increase the open circuit voltage and consequently also efficiency of considered devices. The further CTS modernizing of domestic single crystal Si-SC, in particular, by forming an optimum texture such as "inverted pyramids" on their base crystal front surfaces and BC thinning down to 180–200  $\mu\text{m}$  will provide an additional increase in efficiency and mass-power performance of Si-SC for space applications with  $p$ -type base crystals as well as of Si-SC of terrestrial applications with  $n$ -type base crystals. Thus, as our estimations show, the mass-power performance can be increased in both cases from 200–270 W/kg (the prior

art CTS,  $t = 300 \pm 50 \mu\text{m}$ ) up to 450–500 W/kg (novel CTS).

### References

1. W.Hoffmann, Proc. 17<sup>th</sup> European Photovoltaic Solar Energy Conf., October 22-26, 2001, Munich, Germany, p.851.
2. E.Martinot, Renewables 2005 Global Status Report. Washington, DC: Worldwatch Institute, 80 p.; <http://www.ren.net>.
3. EPIA Roadmap, 2004; <http://www.epia.org>.
4. M.A.Green, K.Emery, D.L.King et al., *Prog. Photovolt.: Res.Appl.*, **14**, 45 (2006).
5. J.Zhao, A.Wang, P.Campbell et al., Proc. 26<sup>th</sup> IEEE Photovoltaic Specialists Conf., September 30-October 3, 1997, Anaheim, CA, p.1133.
6. A.L.Fahrenbruch, R.H.Bube, Fundamentals of Solar Cells. Photovoltaic Solar Energy Conversion, Academic Press, New York (1983).
7. P.Wawer, A.Schmidt, H.-G.Wagemann, Proc. 14<sup>th</sup> European Photovoltaic Solar Energy Conference, June 30-July 4, 1997, Barcelona, Spain, p.2450.
8. S.W.Glunz, S.Rein, W.Warta et al., Proc. 2<sup>nd</sup> World Conf. and Exhibition on Photovoltaic Solar Energy Conversion, July 6-10, 1998, Vienna, Austria, p.1343.
9. J.Schmidt, A.G.Aberle, R.Hezel, Proc 26<sup>th</sup> IEEE Photovoltaic Specialists Conf., September 30-October 3, 1997, Anaheim, CA, p.13.
10. J.Zhao, A.Wang, P.Altermatt et al., *Appl. Phys.Lett.*, **66**, 3636 (1995).
11. R.Ludeman, S.Schaefer, J.Reib, Proc. 2<sup>nd</sup> World Conf. and Exhibition on the Photovoltaic Solar Energy Conversion, July 6-10, 1998, Vienna, Austria, p.3636.
12. V.A.Antonova, V.N.Borshchov, V.R.Kopach et al., *Functional Materials*, **10**, 168 (2003).
13. W.Keogh, A.Cuevas, Proc. 26<sup>th</sup> IEEE Photovoltaic Specialists Conf., September 30-October 3, 1997, Anaheim, CA, p.199.
14. E.Kerschaver, R.Einhaus, J.Szlufcik, Proc. 14<sup>th</sup> European Photovoltaic Solar Energy Conf., June 30-July 4, 1997, Barcelona, Spain, p.2438.

## **Оптимізація базових кристалів для кремнієвих фотоелектричних перетворювачів різного призначення**

***М.В.Кіріченко, І.Т.Тимчук, В.А.Антонова,  
Н.П.Клочко, В.Р.Копач, О.М.Лістратенко***

Наведено результати досліджень спектральної залежності коефіцієнта відбиття  $R(\lambda)$  для різних типів текстури ("інвертовані піраміди" та "V-канавки") фотоприймальної поверхні монокристалічних кремнієвих пластин, а також вихідних та діодних параметрів фотоелектричних перетворювачів (ФЕП) з базовими кристалами (БК) кремнію  $p$ - та  $n$ -типу провідності. На підставі проведеного порівняльного аналізу залежностей  $R(\lambda)$  обгрунтовано вибір оптимального типу текстури фотоприймальної поверхні Si-БК. Шляхом зіставлення вихідних та діодних параметрів ФЕП з Si-БК  $p$ - та  $n$ -типу провідності обгрунтовано доцільність створення високоефективних монокристалічних Si-ФЕП на основі кремнію  $n$ -типу провідності.